Research Square

Preprints are preliminary reports that have not undergone peer review.
They should not be considered conclusive, used to inform clinical practice,
or referenced by the media as validated information.

Saccadic network dysfunction underlies eye-movement variability in early Parkinson's disease

Varsha Vasudevan
Indian Institute of Technology Bombay
Sandy Mournet
Sorbonne Universite, UMR S 1127, Inserm U 1127, CNRS UMR 7225, and Institut du Cerveau et de la Moelle epiniere
Benoît Béranger
Sorbonne Universite, UMR S 1127, Inserm U 1127, CNRS UMR 7225, and Institut du Cerveau et de la Moelle epiniere
Caitlin Paige Rogers
Sorbonne Universite, UMR S 1127, Inserm U 1127, CNRS UMR 7225, and Institut du Cerveau et de la Moelle epiniere
Graziella Mangone
Sorbonne Universite, UMR S 1127, Inserm U 1127, CNRS UMR 7225, and Institut du Cerveau et de la Moelle epiniere
Isabelle Arnulf
Sorbonne Universite, UMR S 1127, Inserm U 1127, CNRS UMR 7225, and Institut du Cerveau et de la Moelle epiniere
Jean-Christophe Corvol
Sorbonne Universite, UMR S 1127, Inserm U 1127, CNRS UMR 7225, and Institut du Cerveau et de la Moelle epiniere
Marie Vidailhet
Sorbonne Universite, UMR S 1127, Inserm U 1127, CNRS UMR 7225, and Institut du Cerveau et de la Moelle epiniere
Stéphane Lehericy
Sorbonne Universite, UMR S 1127, Inserm U 1127, CNRS UMR 7225, and Institut du Cerveau et de la Moelle epiniere
Pierre Pouget
Sorbonne Universite, UMR S 1127, Inserm U 1127, CNRS UMR 7225, and Institut du Cerveau et de la Moelle epiniere
Nivethida Thirugnanasambandam
Indian Institute of Technology Bombay
Cecile Gallea
cecile.gallea.icm@gmail.com

Sorbonne Universite, UMR S 1127, Inserm U 1127, CNRS UMR 7225, and Institut du Cerveau et de la Moelle epiniere

Article

Keywords: Saccades, Parkinson's disease, Variability, Functional connectivity, Network-behavior coupling

Posted Date: November 18th, 2026

DOI: https://doi.org/10.21203/rs.3.rs-11410738/v1

License: This work is licensed under a Creative Commons Attribution 4.0 International License. Read Full License

Additional Declarations: No competing interests reported.

Abstract

Parkinson's disease is a neurodegenerative disorder characterized by altered subcortical-cortical connectivity, leading to motor and cognitive deficits. Saccadic eye movement abnormalities are among the earliest and most persistent markers of the disease, serving as sensitive indicators of disrupted oculomotor and cognitive control. While changes in average saccadic behavioral measures are widely reported in Parkinson's disease, intra-individual variability in saccadic performance and the underlying network dysfunction remain poorly understood. Here, we quantified intra-individual saccadic variability in early-stage Parkinson's disease and identified its functional correlates within the resting-state saccadic network. We analyzed data from the inclusion visit of 91 patients with early-stage Parkinson's disease and 46 healthy controls from the ICEBERG cohort (monocentric prospective research study) who underwent oculomotor testing and resting-state functional magnetic resonance imaging. First, at the behavioral level, we assessed intra-individual variability in saccadic performance within each group using the coefficient of variation of reaction time and normalized peak velocity across trials. Second, at the brain level, we assessed group differences in static and dynamic functional connectivity across 39 regions comprising the saccadic network. We examined the relationship between network connectivity and saccadic variability using partial least squares analysis. We also quantified network organization using graph-theory measures of global efficiency and clustering coefficient. Finally, we tested the relevance of intra-individual saccadic variability and network features in distinguishing patients from healthy controls using a multivariate Mahalanobis classifier. Our results showed that, compared to HC, patients had higher intra-individual variability in saccadic behavioral measures of reaction time (p Holm = 0.012) and normalized peak velocity (p Holm = 0.012). Interestingly, patients had (i) reduced static and dynamic connectivity within the saccadic network and (ii) weaker associations between network connectivity and intra-individual saccadic variability of specifically normalized peak velocity. These results were particularly driven by regions within the cognitive saccade network. The classifier that integrated intra-individual saccadic variability and network connectivity achieved 95.62% accuracy in distinguishing patients from healthy controls, with dynamic connectivity contributing more strongly to classification performance than static connectivity. We demonstrate that elevated intra-individual variability of saccades, underpinned by altered functional connectivity within cognitive-oculomotor networks, is a prominent feature of early-stage Parkinson's disease. Emerging as a promising physiological marker of disease pathophysiology, intra-individual variability offers a powerful new framework to refine early diagnosis and improve the tracking of neurodegeneration before severe clinical milestones are reached.

Introduction

Parkinson's disease (PD) is associated with widespread behavioral deficits spanning multiple domains, including gait, upper-limb coordination, speech, and oculomotor function. Among the earliest and most consistent manifestations of PD are abnormalities in saccadic eye movements, which can predict cognitive decline, gait disturbances, and overall disease progression[1–4]. Beyond mean performance deficits, PD is increasingly recognized as a disorder characterized by heightened intra-individual variability across motor domains[5–11]. These trial-to-trial fluctuations capture dimensions of motor control that average metrics fail to detect, offering a potentially more sensitive index of neurological dysfunction. In particular, intra-individual saccadic variability reflects subtle alterations within the oculomotor system[12–16]. Nevertheless, prior research in PD has overwhelmingly focused on mean performance, leaving trial-to-trial saccadic variability relatively underexplored. Consequently, how saccadic variability relates to underlying brain dynamics in PD remains poorly understood.

Saccade generation relies on a distributed brain network spanning cortical and subcortical regions[17–20]. Precise saccadic control requires synchronized interactions between prefrontal and parietal executive centers and subcortical motor circuits within the basal ganglia, brainstem, and cerebellum[21–23]. Given this distributed topology, the oculomotor system serves as a powerful model for examining how network dynamics govern behavior. While brain function was traditionally mapped using static connectivity, growing evidence underscores the importance of dynamic functional connectivity, i.e., transient reconfigurations in network topology that are uniquely vulnerable to pathological disruption[24–30]. Characterizing the dynamic properties of the saccadic network may therefore yield critical insights into the brain-behavior relationships that govern intra-individual saccadic variability.

Behaviorally, saccadic impairment in PD spans both motor and cognitive domains. Motor deficits encompass reduced accuracy of task performance, higher error rates, and altered kinematics (velocity, amplitude, and duration)[18,31–34], whereas cognitive deficits manifest primarily as increased latencies in saccade planning and initiation[3,35–37]. Although cognitive impairments are well-established[1,36,38–40], the heterogeneity of motor deficits[35,37,41,42] highlights a major gap in our understanding of oculomotor pathophysiology. Given that saccade generation relies on the tight integration of cognitive and motor control[48–50], these behavioral deficits likely arise from large-scale brain network reconfigurations[43–47] within interconnected subcortical and cortical networks[51–53]. Dynamic interactions among cognitive and motor regions may be detrimental or could contribute to the maintenance of motor behavior[54,55] and cognitive performance[30,43]. For instance, PD is characterized by functional reorganization across brain networks during choice tasks involving hand responses[33], where interactions between cognitive and motor nodes may serve as compensatory mechanisms to counteract progressive neurodegeneration. Whether this functional reorganization extends to the saccadic network and directly accounts for eye-movement deficits in PD remains unknown. Specifically, how pathological shifts in dynamic connectivity of the saccadic network contribute to elevated intra-individual saccadic variability has not been established. Furthermore, the relative contributions of the cognitive and motor subdivisions of the saccadic network and their interactions to behavioral variability remain uncharacterized. Elucidating the relationship between dynamic network organization and oculomotor variability may therefore provide critical mechanistic insights into the neural architecture underlying saccadic dysfunction in PD.

The primary objective of this study was to investigate whether altered dynamics within the saccadic network, encompassing both its cognitive and motor sub-circuits, explain intra-individual variability in saccadic behavior in early PD. To test this, we enrolled patients with early-stage PD and age-matched healthy controls, quantifying both behavioral saccadic variability and intrinsic functional connectivity within the saccadic network using static and dynamic resting-state approaches. We tested three primary hypotheses: **(i)** patients with early-stage PD exhibit heightened intra-individual saccadic variability and altered functional connectivity within the saccadic network relative to healthy controls; **(ii)** the coupling between saccadic network connectivity and behavioral variability is altered in PD; and **(iii)** because saccade generation relies on fluctuating, moment-to-moment network reconfigurations, dynamic functional connectivity should better characterize PD than static functional connectivity. We used a low-cognitive-load prosaccade task to evaluate saccadic variability. Although often termed a reflexive response, prosaccades depend on an elegant loop of spatial attention, target selection, and motor execution[20,21,23,56,57]. This methodological choice allowed us to isolate the neural interface between cognitive and motor networks without overloading the oculomotor system that is fragilized in PD patients. By integrating behavioral and neuroimaging metrics, this work advances our systems-level understanding of how cognitive and motor aspects of oculomotor control are disrupted in PD, highlighting its potential utility for early brain/behavior biomarker development.

Materials and methods

Participants and clinical data

The participants in this study were part of the monocentric prospective research cohort study conducted by the Paris Brain Institute between 2014 and 2022 (the ICEBERG study, ClinicalTrials.gov Identifier: NCT02305147). The cohort included healthy participants and individuals with PD, from whom we selected participants who had both oculomotor and neuroimaging recordings at the inclusion visit. The patient inclusion criteria included (i) clinical diagnosis of PD (UK Brain Bank criteria) by sleep neurologists or movement disorder specialists, (ii) age between 18 and 75 years, (iii) no or subtle cognitive impairment (Mini-Mental State Examination score > 26/30), and (iv) time-from-diagnosis ≤ 4 years. Control participants were evaluated through clinical examination to verify the absence of a history of neurological or psychiatric disease. The study was approved by the local ethics committee (CPP Paris VI, RCB: 2014-A00725-42). All participants provided written informed consent, and the research was conducted in accordance with the Declaration of Helsinki. From the large cohort (see details in[58]), we included healthy controls (HC) and PD patients who underwent both MRI and oculomotor testing. Clinical assessment of patients was conducted using standardized scales, including the Movement Disorder Society Unified Parkinson's Disease Rating Scale (MDS-UPDRS), Mini-Mental State Examination (MMSE), and Montreal Cognitive Assessment (MoCA). Oculomotor tests were performed at each visit under dopamine-ON conditions.

Oculomotor data

Data acquisition and paradigm

Participants sat in a dark room with their eyes open in front of a 26-inch LCD monitor (ProLite Iiyama PL2600) at 60 cm (visual angle of 56° × 35°). Stimuli were displayed at 1920 × 1080 pixels and a 144 Hz monitor setting. Eye movements were recorded with a video-based eye tracker (Mobile EBT©, eyeBRAIN, France) at 500 Hz. Before the task, a standard nine-point calibration was conducted, requiring participants to fixate a 0.5° red target for 250 ms at each location. The spatial accuracy was approximately 0.25°- 0.5°, and baseline noise was below 0.5°. The task was controlled using MeyeParadigm software, and eye-movement data were exported via MeyeAnalysis (v1.20.1).

The saccade task (**Supplementary Fig. 1**) started with a central green fixation point (15 × 15 pixels; luminance 120 cd/m²) appearing on a black background (jittered interval of 2500–3500 ms). After a 200 ms gap following the fixation period during which the screen is blank, a red target of the same size appeared at ± 25° along the horizontal meridian. The target location was randomized to the left or right and visible for 1000 ms. Participants were instructed to make a rapid eye movement to the target, then return to the central fixation for the next trial. Each participant performed 48 horizontal saccades in two or four blocks.

Data analysis

Oculomotor data were analyzed using MATLAB scripts (R2023a, MathWorks, MA, USA). Horizontal and vertical eye position signals were segmented into trials using event markers corresponding to fixation onset and target onset. Trial boundaries were defined from fixation onset to the onset of the subsequent trial. All trials to both left and right targets were combined and analyzed. Position signals were smoothed using a Savitzky–Golay filter (order = 5, frame length = 21 samples). Trial-wise baseline drift was removed by subtracting the mean eye position computed over a 20-ms window immediately preceding target onset. Angular displacement was calculated from the drift-corrected horizontal and vertical components. Velocity was obtained using Savitzky–Golay differentiation kernels.

Saccades were detected using a velocity-based algorithm. For each trial, the peak velocity following target onset was identified, and saccade onset and offset were defined as the first and last time points at which velocity crossed 10% of the peak velocity before and after the peak, respectively. Reaction time was the interval between target onset and saccade onset. Trials were excluded if (a) saccade duration exceeded 200 ms, (b) signals showed saturation or flat-line artifacts, (c) baseline was unreliable, or (d) blink artifacts were present during saccade. For all valid trials, we extracted saccade amplitude, peak velocity, reaction time, and duration. Outliers were identified for each parameter using a ± 3-standard-deviation criterion relative to the subject-specific mean and were excluded from further analyses. Trials were concatenated across blocks before subject-level analyses.

We quantified reaction time as a measure of saccadic decision-making and normalized peak velocity as a marker of saccadic kinematic change. For each participant, we computed the mean and variance across trials for reaction time, amplitude, peak velocity, and duration. To account for the main-sequence relationship between saccade amplitude, duration, and peak velocity, a subject-specific linear regression without intercept was fitted between amplitude and the product of peak velocity and duration[59]. The resulting slope parameter was used to generate predicted peak velocity values, and a normalized peak velocity (NormPV) was computed as a ratio of the observed to predicted peak velocity. The mean and variance of NormPV were then computed at the subject level. To quantify intra-individual saccadic variability relative to mean performance, the coefficient of variation (CV) was calculated as the standard deviation divided by the mean for reaction time and normalized peak velocity (CV-RT and CV-NormPV, respectively). These subject-level behavioral measures were used for subsequent group-level statistical analyses.

Neuroimaging data

Data acquisition

MRI data were acquired for all participants using a 3T Siemens Prisma scanner (Siemens Healthineers, Erlangen, Germany) equipped with a 64-channel head coil. High-resolution structural images were obtained using a T1-weighted three-dimensional MP2RAGE sequence (TR = 5000 ms, TE = 2.98 ms, voxel size = 1 × 1 × 1 mm^3). Resting-state functional images were collected using a multiband single-shot gradient-echo echo-planar imaging sequence (TR = 2190 ms, TE = 25 ms, flip angle = 90°, voxel size = 2.8 mm isotropic, 44 interleaved slices, multiband acceleration factor = 210 volumes). In addition, a shortblipped EPI acquisition (6 volumes) with reversed phase encoding was acquired to enable geometric distortion correction.

Data analysis

Functional MRI preprocessing was performed using Statistical Parametric Mapping (SPM12; Wellcome Trust Center for Neuroimaging, London, UK) implemented in MATLAB. Preprocessing steps included distortion and slice-timing correction, realignment for head-motion correction, artifact detection (ART-based identification with outlier scrubbing), spatial normalization to the Montreal Neurological Institute (MNI) template using DARTEL, and spatial smoothing with a 6-mm full-width-at-half-maximum Gaussian kernel.

Residual BOLD volumes were obtained by fitting a general linear model with nuisance regressors including white matter and cerebrospinal fluid signals, 24 motion parameters (six rigid-body motion parameters and their temporal derivatives and squared terms), and stick regressors identifying volumes with framewise displacement exceeding 0.5 mm and physiological confounds to write the residuals as cleaned 4D volumes. These cleaned volumes were then temporally band-pass filtered (0.01–0.1 Hz) using a fast Fourier transform–based approach to remove low-frequency drift and high-frequency physiological noise.

Region-of-interest (ROI) time series were extracted using custom MATLAB scripts built on SPM12. A predefined saccade network comprising 39 ROIs (**Supplementary Table 1**) was defined based on prior studies and meta-analyses examining the cortical and subcortical networks underlying pro-saccade generation[19,60–68]. ROIs encompassed frontal and parietal cortices, basal ganglia, cerebellar, brainstem, and thalamic structures. The ROIs were defined as described in the Supplementary Methods (subsection - Regions of Interest). Each ROI mask in MNI space was resliced to the functional image space, and the representative time series for each ROI was computed as the first eigenvariate of the voxel time series within the ROI mask using singular value decomposition, capturing the dominant pattern of coherent BOLD activity in the region.

The saccade network (defined using 39 ROIs) was subdivided using an operational functional classification into cognitive ROIs (ROIs 1–15 in **Supplementary Table 1**) comprising regions implicated in saccadic decision-making and higher-order control, and motor ROIs (ROIs 16–39 in **Supplementary Table 1**) comprising regions primarily involved in oculomotor execution and kinematic control. This operational division was based solely on functional roles described in prior studies[57,69–73].

Functional connectivity

We computed the magnitude of communication between two nodes, i.e., their weighted statistical synchronization using Pearson's correlation. We computed the dynamic connectivity matrix for each participant using a sliding-window approach[74]. A window length of 120 seconds was used (window size = round (120/TR) = 55 time points; TR = 2.19 s). Although longer than the typically used windows, this choice ensured reliable sampling of low-frequency dynamics and reduced spurious variability in sliding-window correlations, based on theoretical considerations of signal reliability[75]. We analyzed 220 time windows, each including 55 time points and centered on the middle time point (symmetric window). At scan boundaries, windows were zero-padded to preserve a constant window length. Within each window, pairwise Pearson correlations among all 39 ROI time series were computed, resulting in 1521 edges (derived from 39 ROIs; 39 × 39 = 1521). The analysis yielded a time-resolved 3D connectivity matrix for each subject (39*39*220), with one correlation value per connection at each time window. The dynamic connectivity matrices were Fisher-z transformed. For dynamic connectivity (DC), the Fisher z-transformation was applied at each time window. The matrices were subsequently thresholded using a permutation-based null model derived from temporally shuffled time series[76,77]. For each subject, ROI time series were independently permuted along the temporal dimension, preserving amplitude distributions while disrupting temporal dependencies. To construct the null model, ROI time series were shuffled independently for each region and permutation (1000 iterations per subject). A correlation matrix was computed for each permuted dataset, and the resulting matrices were Fisher-z-transformed. The resulting Fisher-z-transformed coefficients were aggregated across permutations to

generate a subject-specific null distribution of connectivity strengths. A pooled null distribution was then obtained by combining values across all subjects. The statistical threshold was defined as the 95th percentile of this pooled null distribution. Weighted adjacency matrices were constructed by retaining suprathreshold Fisher z-values and setting subthreshold connections to zero. For time-resolved DC, the same threshold was applied at each time window to derive dynamic adjacency matrices.

The functional connectivity matrix was partitioned into within- and between-network components based on the anatomical classification of the ROIs. Connectivity among the cognitive ROIs (ROIs 1–15) was defined as the cognitive saccade network (CSN), whereas connectivity among the motor ROIs (ROIs 16–39) was defined as the motor saccade network (MSN). Connectivity between the cognitive and motor ROIs was defined as the cognitive-motor saccade network (CMSN). Thus, CSN and MSN represent intra-network connectivity, while the CMSN represents inter-network connectivity (see **Supplementary Fig. 2**).

The computation, thresholding, and analysis of static functional connectivity are described in the Supplementary Methods (subsection - Static connectivity).

Saccadic network-behavior coupling

To quantify the contribution of saccadic network connectivity to behavioral variability, we performed partial least squares regression using functional connectivity measures as predictors and behavioral variability measures as responses. Separate analyses were conducted to evaluate the relative contributions of intra-network (CSN and MSN) and inter-network (CMSN) connectivity. We also assessed whether these saccadic network-behavior relationships differed between HC and PD groups.

We considered DC network measures to investigate the contribution of the saccadic network in explaining the behavioral variability of saccades. Network-behavior coupling was examined using partial least squares (PLS) regression. Predictor variables in the network comprised the vector of correlation coefficients from the upper triangle of the connectivity matrix (n = 741, since it was symmetric) for all subjects in a group, and the behavioral variables CV-NormPV and CV-RT for the subjects. Separate models were estimated for the HC and PD groups. The regression coefficients obtained from the fitted models were used to quantify the strength and direction of coupling between the network connectivity and saccadic variability. These saccadic network- behavior coupling values were then compared between HC and PD to assess disease-related alterations in the saccadic network's contribution to behavioral variability.

Contribution of the cognitive and motor saccade networks

To determine the relative contributions of CSN, MSN, and CMSN, PLS regression was independently refit for each network, using only the edges within that network as predictors. The resulting network-specific connectivity-behavior coupling coefficients were then compared between HC and PD to assess disease-related alterations in each network's contribution to saccadic behavioral variability.

The analogous method for static functional connectivity is described in the Supplementary Methods (subsection - Static connectivity).

Network organization characterization

To quantify the saccadic network organization, we computed graph-theoretical measures using functions from the Brain Connectivity Toolbox (Version 2019-03-03). Executing a saccade requires an optimal balance between (i) local network segregation with specialized processing in distinct networks, which we captured by measuring the clustering coefficient, and (ii) global network integration with rapid data sharing across networks, which we captured by measuring the global efficiency. Before estimating clustering coefficients, the weight matrices were normalized to the range [0,1]. Analyses were performed separately for static connectivity (SC) and dynamic connectivity (DC) matrices without thresholding. Static graph metrics consisted of a single value per subject, derived from subject-specific weighted adjacency matrices, whereas dynamic graph metrics were computed on each time-resolved weighted adjacency matrix. The subject-level values for DC were defined as the mean of the metric computed across all time windows. All graph metrics were computed at the subject level and subsequently used for group-level statistical comparisons between HC and PD patients.

Multivariate classification of PD

We tested whether intrinsic resting-state functional connectivity and saccadic behavioral variability serve as biomarkers of early PD. If so, connectivity- and behavior-derived variables should reliably distinguish PD patients from HC. To test this, we performed multivariate classification using features that showed significant group differences in prior analyses.

We derived global network measures from the entire saccade network, including cognitive and motor components. We reduced connectivity matrices to single-subject-level measures representing overall connectivity strength. For static connectivity, the overall connectivity strength was calculated as the mean of all upper-triangular values of each subject's SC matrix (SC-avgcorr). For dynamic connectivity, we calculated overall connectivity strength as the mean of the upper-triangular values of each subject's dynamic mean connectivity matrix (DC-avgcorr).

Classification was performed using eight subject-level features: static and dynamic overall connectivity strength (SC-avgcorr, DC-avgcorr), static and dynamic clustering coefficients (SC-CC, DC-CC), static and dynamic global efficiencies (SC-Eff, DC-Eff), and behavioral variability measures (CV-NormPV, CV-RT). All features were z-scored across participants before analysis. Classification was implemented using a Mahalanobis distance–based nearest-centroid classifier[78,79] which accounts for differences in feature variance and covariance and is therefore well suited to heterogeneous group

dispersion. Group centroids and covariance matrices were estimated for each group, and each subject was assigned to the group yielding the smaller Mahalanobis distance. Performance was quantified using classification accuracy and receiver operating characteristic (ROC) analysis with area under the curve (AUC). Robustness was assessed using leave-one-out cross-validation (LOOCV), and feature contributions were evaluated via leave-one-feature-out ablation analyses, with LOOCV performance recomputed after each ablation.

Statistical analysis

All statistical analyses were performed in MATLAB (R2023a, MathWorks, MA, USA). There was no missing data, as we selected cohort participants who had both oculomotor and neuroimaging recordings. Statistical significance was set at $p < 0.05$ (two-tailed) unless otherwise specified. For subject-level behavioral measures (reaction time and normalized peak velocity) and graph metrics (clustering coefficient and global efficiency from SC and DC matrices), normality was assessed using the Lilliefors test. Between-group differences (HC vs PD) were evaluated using independent-samples *t*-tests when both groups were normally distributed, and Wilcoxon rank-sum tests otherwise. Test statistics are reported as *t*- or *z*-values, as appropriate.

For group-level statistical comparisons of the connectivity matrices, we used non-parametric permutation testing. We averaged the weighted adjacency matrices across time windows to obtain the DC mean matrix for each subject. These subject-wise average connectivity measures were then used for group-level statistical comparisons. The upper-triangle values of the DC mean matrix of each subject were used. To calculate observed group differences, we combined these values across all ROIs for all subjects within a group (HC or PD) to form a group-specific distribution and then assessed statistical differences using the Wilcoxon rank-sum test. To obtain empirical p-values, group labels were randomly permuted 10000 times while preserving group sizes. For each permutation, the rank-sum statistic was recomputed, and the empirical P-value was calculated as the proportion of permuted statistics equal to or more extreme (95th percentile) than the observed statistic. When no permutation exceeded the observed statistic, P was set to 1/10000.

In both the whole saccadic network and individual CSN, MSN, and CMSN analyses, we assessed within-group reliability of the coupling between network connectivity and saccadic behavior using bootstrap resampling. Between-group differences were tested using a subject-level group-label permutation of group labels, thereby accounting for the dependence among connectivity edges estimated from a single fitted model (for further details, see Supplementary Methods subsection - Dynamic network connectivity to saccadic behavior coupling). Holm-Bonferroni correction (p_{Holm}) was applied within each family of behavioral comparisons to account for multiple comparisons.

Results

Participants and clinical data

Demographics for the 46 HC and 91 PD patients are shown in Table 1. The patient and healthy groups were age-matched, with an imbalanced gender ratio representative of the higher prevalence of PD in males [80,81]. Other than MMSE, which showed a weak trend toward lower scores in PD, and saccade amplitude, which was significantly reduced in PD ($z = 4.86$; $p < 0.001$), no other demographic, cognitive, or saccadic metric differed between groups.

Table 1
Clinical demographics and average metrics of saccadic behavior

Age (mean ± SD[#], years)	**HC (n = 46)**	**PD (n = 91)**
	60.9 ± 9.3	**62.38 ± 9.5**
Sex: male/female (ratio)	22/24 (0.9)	56/35 (1.6)
Disease duration (years)	-	1.22 ± 1.0
Levodopa dose equivalent	-	300.0 ± 125.6
Hoehn and Yahr score	-	2.0 ± 0.2
UPDRS III – "best-on" condition	-	27.0 ± 7.1
[##]MMSE (0–30)	**29.4 ± 0.9**	**29.0 ± 1.0**
MoCA (0–30)	28.5 ± 2.0	28.0 ± 2.0
Saccade reaction time (ms)	234.6 ± 32.2	228.3 ± 32.1
[###]Saccade amplitude (°)	**21.9 ± 1.0**	**20.7 ± 1.4**
Saccade duration (ms)	76.5 ± 11.5	74.9 ± 10.9
Saccade peak velocity (°/s)	457.4 ± 65.0	447.6 ± 55.7

[#]SD: standard deviation; **significant differences are shown in bold;** [##]ranksum, $z = 1.98$, $p = 0.048$; [###]ranksum, $z = 4.86$, $p < 0.001$.

Saccadic behavior changes with PD

Saccadic behavior, quantified as CV-NormPV and CV-RT, combined measures of mean and variance in normalized peak velocity and reaction time, respectively (as described in the Methods), differed between PD and HC. CV-NormPV, which captured the combined effect of amplitude, duration, and peak velocity, significantly increased for PD patients (data distribution: non-normal, rank-sum: $z = -2.51$, $p = 0.012$, $p_{Holm} = 0.012$, Fig. 1A). The CV was significantly higher for reaction time also in PD patients (data distribution: normal, t-test: $t = -2.81$, $p = 0.006$, $p_{Holm} = 0.012$, Fig. 1B). Separate analysis of the differences in mean and variance showed that the CV difference was driven by the significant difference in variance between HC and PD for both normalized peak velocity (rank-sum: $z = -2.53$, $p = 0.011$) and reaction time (rank-sum: $z = -2.25$, $p = 0.024$). There was no significant difference in the means of normalized peak velocity (rank-sum: $z = -0.52$, $p = 0.605$) or reaction time (t-test: $t = 1.10$, $p = 0.274$) between the groups. Interestingly, the variability was greater in magnitude for reaction time than for normalized peak velocity.

Saccadic network connectivity changes in PD

Both SC and DC were lower in PD, as shown by the group-averaged global network measure, i.e., the average connectivity across all edges of the connectivity matrix of the whole saccadic network (Fig. 2A). The edgewise difference in the mean DC calculated across the time windows revealed a distributed pattern across the saccadic network ROIs in the group differences obtained using a non-parametric label-permutation approach (n = 10000, 95th percentile threshold = 0.0314). Of the total 741 edges in the upper half of the connectivity matrix excluding the diagonal, 515 edges (69.5%) showed significant differences, most of which (99.8%) had reduced DC in PD (Fig. 2B). SC also yielded similar group differences (**Supplementary Fig. 3**). Of the 515 edges that showed significantly reduced connectivity in PD, the largest proportion involved the CSN (42.5%), followed by the MSN (28.2%) and CMSN (29.2%). Only 1.3% of altered edges showed increased connectivity in the PD group, primarily in the MSN. These findings indicate a widespread reduction in connectivity across the saccadic network in PD, affecting all three functional subnetworks, with the largest proportion of altered connections involving the CSN.

Saccadic network - behavior coupling

The partial least squares regression analysis used 741 connectivity values from the upper half of the connectivity matrices to predict two behavioral measures (CV-NormPV and CV-RT) in HC and PD separately. Here, we highlight the results of analyses using DC measures. Analyses using SC measures yielded similar results (**Supplementary Fig. 4**).

Saccadic network contribution to intra-individual saccadic variability: In HC, the connectivity pattern of the saccadic network explained CV-NormPV and CV-RT differently from PD (Fig. 3A and 3B, radial lines, blue - HC and red - PD). Higher connectivity was reliably associated with greater CV-NormPV ($p = 0.002$, $p_{Holm} = 0.005$; Fig. 3C, blue violin), while network connectivity was unrelated to CV-RT ($p = 0.77$, $p_{Holm} = 0.77$; Fig. 3D, blue violin). In contrast, network connectivity in PD patients showed no reliable relationship to either measure of saccadic variability (CV-NormPV: $p = 0.49$, $p_{Holm} = 0.54$; CV-RT: $p = 0.54$, $p_{Holm} = 0.54$; Fig. 3C-D, red violins). Comparing PD and HC, mean network-behavior coupling differed significantly between groups for CV-NormPV ($p = 0.01$, $p_{Holm} = 0.02$), but not for CV-RT ($p = 0.17$, $p_{Holm} = 0.17$). Full statistical details for the within-group and between-group analyses are provided in **Supplementary Table 2**.

Contribution of cognitive and motor saccadic networks and their interactions to intra-individual saccadic variability. In HC and PD, network-behavior coupling followed different trends across all three saccade networks of CSN, MSN, and CMSN (Fig. 4A-C). Within HC, connectivity showed a significant coupling to CV-NormPV in CSN (bootstrap resampling, $p = 0.02$, $p_{Holm} = 0.02$), MSN (bootstrap resampling, $p = 0.006$, $p_{Holm} = 0.017$), and CMSN (bootstrap resampling, $p = 0.006$, $p_{Holm} = 0.017$). This coupling was disrupted in PD, with no network connectivity showing a reliable relationship to CV-NormPV (CSN: $p = 0.19$, $p_{Holm} = 0.59$; MSN: $p = 0.81$, $p_{Holm} = 1.00$; CMSN: $p = 0.76$, $p_{Holm} = 1.00$). Comparing HC and PD directly, the between-group difference in coupling to CV-NormPV was significant only for CSN (group-label permutation, $p = 0.006$, $p_{Holm} = 0.017$) and did not reach significance for MSN ($p = 0.07$, $p_{Holm} = 0.07$). For CMSN, although there was a significant trend, this did not survive correction for multiple comparisons ($p = 0.03$, $p_{Holm} = 0.06$). For CV-RT, none of the within-group or between-group comparisons were significant (all $p_{Holm} \geq 0.37$). The detailed statistics for all comparisons are presented in **Supplementary Table 3**.

Overall, saccadic network connectivity showed a reliable relationship with peak-velocity variability in HC that was absent in PD, both at the whole-network level and consistently across all three networks of CSN, MSN, and CMSN. The cognitive saccade network (CSN) showed the only significant between-group difference. No comparable relationship was detected for reaction-time variability at any level of analysis in either group.

Network organization changes with PD

The reorganization of saccadic network topology was quantified using graph metrics. Significant group differences were observed in metrics derived from both SC and mean DC (Fig. 5A-D). The clustering coefficient was lower in PD for both SC and DC connectivity (SC: t-test, $t = 2.85$, $p = 0.005$, $p_{Holm} = 0.012$; DC: rank-sum, $z = 2.76$, $p = 0.006$, $p_{Holm} = 0.012$; Fig. 5A, C). Similarly, PD patients had reduced global efficiency (SC: t-test, $t = 2.94$, $p = 0.004$, $p_{Holm} = 0.012$; DC: t-test, $t = 3.07$, $p = 0.003$, $p_{Holm} = 0.010$; Fig. 5B, D).

Multivariate classification of Parkinson's disease

The classifier built using all 8 features representing network connectivity strength and organization, as well as behavioral variability, achieved a high classification accuracy of 98.5%, with only 2 HC individuals misclassified as PD patients (Fig. 6A). The LOOCV, used to assess model generalizability to

unseen individuals, yielded a classification accuracy of 95.6%, indicating robust and stable group separability across subjects. ROC curves and the full model exhibited near-ceiling performance, with high true positive rates achieved at very low false positive rates, confirming robust separability in the multivariate feature space (see bold black ROC curve in Fig. 6B). The ROC performance degraded the most upon the removal of DC-based averaged connectivity strength (DC-avgcorr; see the downward shift of the dashed blue ROC curve compared to the bold black curve in Fig. 6B). The ablation analyses showed that classification accuracy decreased to 61.3% when only DC features were removed, and to 83.9% when only SC features were removed (Fig. 6C). In summary, the multivariate feature set showed robust separation of PD and HC, with DC connectivity strength contributing more strongly to classification than SC connectivity.

Discussion

In this study, we demonstrate that early-stage PD is characterized by a distinct threefold signature of elevated intra-individual saccadic variability, intrinsic saccadic network degradation, and decoupled brain-behavior interactions. Specifically, patients exhibited marked increases in saccadic variability accompanied by reduced functional connectivity within the saccadic network. Crucially, the breakdown in network-behavior coupling was primarily driven by functional reorganization within the cognitive areas primarily involved in oculomotor movement generation. At the topological level, graph-theoretical analyses revealed pervasive network disintegration, marked by diminished segregation and integration. Consequently, combining dynamic network properties with behavioral intra-individual variability robustly discriminates patients with PD from healthy controls. Collectively, these findings establish oculomotor intra-individual variability and dynamic network architecture as sensitive systems-level markers of early neurodegeneration.

Intra-individual variability represents a robust behavioral marker of saccadic impairment in early-stage PD. Our findings demonstrate that trial-to-trial saccadic variability may be a more sensitive feature explained by disrupted functional network connectivity, unlike mean saccadic performance, which may primarily reflect average neural activity and can therefore remain relatively preserved through compensation. These results support the emerging paradigm that behavioral variability reflects the stochastic dynamics of sensory, cognitive, and motor processing[82–84] within intrinsically noisy neural systems. Rather than being dismissed as mere statistical noise, behavioral variability serves as an informative indicator of motor network integrity[85]. Within the oculomotor system, where kinematics are rapid and exquisitely quantifiable, intra-individual variability provides a sensitive window into central sensorimotor control[15,16]. Consistent with previous studies in PD[67,86–88], patients exhibited marked increases in the variability of reaction time and peak velocity. Notably, the coefficient of variation for both reaction time and normalized peak velocity robustly differentiated patients with PD from healthy controls, even in the absence of significant differences in mean performance. Preserved mean performance may be maintained through transient compensatory mechanisms that obscure underlying network degradation, likely explaining the inconsistent findings in mean saccadic metrics reported across PD cohorts[89–92]. Similar increases in behavioral variability across distinct neurological disorders[93–96] and effector systems[97–100] suggest that heightened movement variability reflects a universal hallmark of pathological neural instability. Consequently, these findings reinforce the necessity of treating intra-individual variability not as residual noise, but as a robust, clinically meaningful dimension of neurodegenerative disease characterization.

Altered saccadic network dynamics represent a fundamental neurobiological hallmark of early-stage PD. In this study, we confirmed the hypothesis that PD is characterized by disrupted brain dynamics across interconnected neural systems. Although historically conceptualized primarily as a focal dopaminergic pathology, converging evidence now situates PD as a primary model of large-scale network dysregulation[86,101–105]. Our findings extend this network perspective to the oculomotor system, demonstrating that disease-related dysfunction reflects a widespread reorganization of cognitive and motor nodes across cortical and subcortical regions. While previous oculomotor research in PD has predominantly focused on regional activation differences or whole-brain alterations[50,62,106], the primary novelty of the present work lies in characterizing how these specialized nodes interact as a coordinated system. Using functional connectivity and graph-theoretical metrics, we demonstrated pervasive reductions in saccadic network connectivity accompanied by decreased global efficiency and clustering coefficients. This pattern indicates a dual impairment in global integration and local segregation across the saccadic network, a system-level disintegration that remains undetectable when evaluating regional activity alone.

Whereas most resting-state functional connectivity studies in PD have relied on static correlations[102,107–110], our findings highlight the critical added value of dynamic functional connectivity[111–114]. Dynamic metrics capture time-varying fluctuations in connectivity, serving as a proxy for network-level neural communication variability. This approach aligns with dynamical-systems frameworks of brain function, which posit that neural activity evolves over time within structured state spaces constrained by underlying anatomical architecture[115]. Within this framework, large-scale brain networks exhibit attractor landscapes that govern transitions between stable functional states; dynamic connectivity thus indexes how the brain traverses these energy landscapes[116]. In PD, the disruption of such dynamics manifests as (i) lower efficiency of communication reflecting reduced neural flexibility; and (ii) reduced clustering coefficient reflecting uncoupled coordination within the saccadic network nodes. Thus, this drives saccadic network-level disintegration and confers high sensitivity for disease classification. Future research quantifying transient network states, dwell times, and transition topologies in behaviorally grounded networks will be essential for uncovering the covert neural mechanisms driving subtle clinical manifestations.

Functional reorganization of the cognitive-motor network represents a hallmark of early-stage PD. By combining neuroimaging and oculomotor behavior in patients with early-stage PD, we demonstrate that disrupted functional connectivity directly underlies elevated intra-individual variability in saccadic behavior. In healthy controls, functional connectivity within cognitive and motor saccadic sub-networks was reliably associated with normalized peak velocity variability, while showing no association with reaction time variability, illustrating that behavioral stability of saccade kinematics depends on fine-tuned, coordinated network interactions. This aligns with prior literature describing decision-making and kinematic

processes as tightly coupled within an integrated cognitive-motor architecture[117–120]. In PD, however, this coordinated brain-behavior topology was fundamentally altered, with network-behavior coupling to normalized peak velocity variability lost across the cognitive and motor networks and their interaction. This loss of coupling was robustly driven by the cognitive saccadic network, reflecting network-level disruption and partial functional reorganization. By decomposing the saccadic network into its constituent cognitive and motor sub-circuits, we uncovered the distinct contributions of these sub-networks to trial-to-trial behavioral variability, reinforcing the concept that behavioral variability is shaped by large-scale network architecture and is exquisitely sensitive to neurodegenerative pathology[121–123].

In early-stage PD, functional alterations were most prominent within the cognitive saccadic network and extended across inter-network connections. This finding accords with the notion that cognitive control recruits distributed inter-network interactions (including recruitment of motor circuits)[124–126] to support compensatory processes that preserve motor output despite progressive motor network degradation. Indeed, longitudinal neuroimaging evidence indicates that PD progression is shaped by dynamic cerebral compensation, wherein increased engagement of parieto-premotor circuits helps offset emerging motor deficits such as bradykinesia[127]. In this context, the altered coupling between saccadic variability and the cognitive sub-network (contrasted with the relative stability of the motor sub-network) could reflect an active compensatory mechanism. Collectively, these findings position cognitive-motor network reorganization as a pivotal systems-level bridging mechanism, linking altered neural dynamics to behavioral dysfunction in PD. Future studies could investigate whether non-invasive neuromodulation could serve as a targeted therapeutic tool to restore network-behavior coupling and rehabilitate motor stability.

Several methodological limitations of the present study warrant consideration. First, functional connectivity estimates were derived from resting-state functional MRI rather than task-based paradigms, which limits direct inference regarding online neural dynamics during active saccade generation. Second, all patients were evaluated in the dopaminergic ‘ON’ state; consequently, potential treatment-induced effects on both behavioral variability and network connectivity cannot be entirely ruled out. Third, although our machine-learning model achieved robust classification performance, external validation in larger, independent cohorts will be essential to establish the generalizability and clinical utility of eye-movement intra-individual variability and dynamic connectivity as robust markers of early PD. Finally, the observed imbalance in sex distribution between groups may have introduced subtle confounding influences on network topology and motor variability. Further studies utilizing larger, sex-stratified cohorts will be necessary to explicitly dissociate sex-specific effects from disease-related pathophysiological mechanisms.

In conclusion, this study establishes a clinical framework for brain–behavior integration in early-stage PD. Rather than reflecting isolated neural or behavioral deficits, PD manifests as a system-level disruption across interconnected networks. While separate individual behavioral or neuroimaging metrics provide incomplete clinical insights, their integration robustly distinguishes patients with PD from healthy controls. Saccadic eye movements represent an ideal translational tool: they are rapid, non-invasive, scalable, and probe distributed cortical–subcortical networks susceptible to neurodegenerative processes[56,128–131]. Combining saccadic variability with intrinsic network connectivity offers significant potential for early disease detection before overt clinical presentation, as well as for the differential diagnosis of atypical parkinsonian syndromes with distinct brainstem and cerebellar involvement[127]. Ultimately, because oculomotor dysfunction tracks key prognostic indicators (including freezing of gait and cognitive decline)[3,11,132–134], behaviorally anchored network dynamics could establish a robust foundation for phenotyping, stratifying, and monitoring parkinsonian disorders.

Data availability

The data supporting the findings of this study are not publicly available due to ethical and privacy restrictions involving human participant data. Aggregated data may be available from the corresponding author upon reasonable request and subject to institutional approval.

Declarations

Competing interests

The authors report no competing interests.

Author Contribution

CG, PP, IA, MV, JCC and SL conceptualized and designed the study. GM performed data collection. CG, SM, VV, BB and CPR performed data curation. VV, BB and CPR carried out the formal analysis. CG, NT and VV were responsible for the writing of the manuscript (original draft preparation). CG, NT and PP provided supervision. SL, MV, JCC were responsible for project administration. All authors read and agreed to the published version of the manuscript, with CG, NT, PP, SL, MV, JCC, and IA performing critical review and editing.

Acknowledgement

The ICEBERG study was funded by grants from the Investissements d’Avenir, IAIHU-06 (Paris Institute of Neurosciences – IHU), ANR-11-INBS-0006, Fondation d’Entreprise EDF, Biogen Inc., JPND Control-PD (ANR-21-JPW2-0005-05), Fondation Thérèse and René Planiol, Fondation Saint Michel,

Energipole (M. Mallart), M. Villain, and the Société Française de Médecine Esthétique (M. Legrand).

Data Availability

The data supporting the findings of this study are not publicly available due to ethical and privacy restrictions involving human participant data. Aggregated data may be available from the corresponding author upon reasonable request and subject to institutional approval.

References

1. Stuart S, Lawson RA, Yarnall AJ, et al. Pro-Saccades Predict Cognitive Decline in Parkinson's Disease: ICICLE-PD. *Mov Disord*. 2019;34(11):1690–1698. doi:10.1002/mds.27813
2. Wang M, Li Y, Yao J, et al. Memory-guided saccade latency as a potential biomarker for axial symptoms and freezing of gait in Parkinson's disease. *Neurobiol Dis*. 2026;218:107238. doi:10.1016/j.nbd.2025.107238
3. Gallea C, Wicki B, Ewenczyk C, et al. Antisaccade, a predictive marker for freezing of gait in Parkinson's disease and gait/gaze network connectivity. *Brain*. 2021;144(2):504–514. doi:10.1093/brain/awaa407
4. Morrison S, Moxey J, Reilly N, Russell DM, Thomas KM, Grunsfeld AA. The relation between falls risk and movement variability in Parkinson's disease. *Exp Brain Res 2021 2397*. 2021;239(7):2077–2087. doi:10.1007/S00221-021-06113-9
5. Barbe MT, Amarell M, Snijders AH, et al. Gait and upper limb variability in Parkinson's disease patients with and without freezing of gait. *J Neurol 2013 2612*. 2013;261(2):330–342. doi:10.1007/S00415-013-7199-1
6. Hausdorff JM, Cudkowicz ME, Firtion R, Wei JY, Goldberger AL. Gait variability and basal ganglia disorders: stride-to-stride variations of gait cycle timing in Parkinson's disease and Huntington's disease. *Mov Disord*. 1998;13(3):428–437. doi:10.1002/MDS.870130310
7. Ko NH, Laine CM, Fisher BE, Valero-Cuevas FJ. Dynamic Fingertip Force Variability in Individuals With Parkinson's Disease. *J Hand Ther*. 2016;29(2):e8. doi:10.1016/j.jht.2016.02.020
8. Park J, Jo HJ, Lewis MM, Huang X, Latash ML. Effects of Parkinson's disease on optimization and structure of variance in multi-finger tasks. *Exp Brain Res* 2013 *2311*. 2013;231(1):51–63. doi:10.1007/S00221-013-3665-3
9. Ko NH, Laine CM, Fisher BE, Valero-Cuevas FJ. Force variability during dexterous manipulation in individuals with mild to moderate Parkinson's disease. *Front Aging Neurosci*. 2015;7(JUL):151948. doi:10.3389/FNAGI.2015.00151/TEXT
10. Baik K, Byun S, Kwag S, et al. Saccadic variability in patients with Parkinson's disease. *J Neurol 2026 2733*. 2026;273(3):197-. doi:10.1007/S00415-026-13733-0
11. Nemanich ST, Earhart GM. Freezing of gait is associated with increased saccade latency and variability in Parkinson's disease. *Clin Neurophysiol*. 2016;127(6):2394. doi:10.1016/j.clinph.2016.03.017
12. Harris CM, Wolpert DM. Signal-dependent noise determines motor planning. *Nat 1998 3946695*. 1998;394(6695):780–784. doi:10.1038/29528
13. Herman JP, Cloud CP, Wallman J. End-Point Variability Is Not Noise in Saccade Adaptation. *PLoS One*. 2013;8(3):e59731. doi:10.1371/JOURNAL.PONE.0059731
14. Beers RJ van. The Sources of Variability in Saccadic Eye Movements. *J Neurosci*. 2007;27(33):8757 LP – 8770. doi:10.1523/JNEUROSCI.2311-07.2007
15. Vasudevan V, Murthy A, Padhi R. Modeling kinematic variability reveals displacement and velocity based dual control of saccadic eye movements. *Exp Brain Res 2024 2429*. 2024;242(9):2159–2176. doi:10.1007/S00221-024-06870-3
16. Eggert T, Robinson FR, Straube A. Modeling Inter-trial Variability of Saccade Trajectories: Effects of Lesions of the Oculomotor Part of the Fastigial Nucleus. *PLOS Comput Biol*. 2016;12(6):e1004866. doi:10.1371/JOURNAL.PCBI.1004866
17. Ettinger U, Kumari V, Crawford TJ, Davis RE, Sharma T, Corr PJ. Reliability of smooth pursuit, fixation, and saccadic eye movements. *Psychophysiology*. 2003;40(4):620–628. doi:10.1111/1469-8986.00063;ISSUE:ISSUE:DOI
18. Kowler E, Blaser E. The accuracy and precision of saccades to small and large targets. *Vision Res*. 1995;35(12):1741–1754. doi:10.1016/0042-6989(94)00255-K
19. Coiner B, Pan H, Bennett ML, et al. Functional neuroanatomy of the human eye movement network: a review and atlas. *Brain Struct Funct*. 2019;224(8):2603–2617. doi:10.1007/s00429-019-01932-7
20. Munoz DP. Commentary: Saccadic eye movements: overview of neural circuitry. *Prog Brain Res*. 2002;140:89–96. doi:10.1016/S0079-6123(02)40044-1
21. Lynch JC, Tian JR. Cortico-cortical networks and cortico-subcortical loops for the higher control of eye movements. *Prog Brain Res*. 2006;151:461–501. doi:10.1016/S0079-6123(05)51015-X
22. Sparks DL. The brainstem control of saccadic eye movements. *Nat Rev Neurosci 2002 312*. 2002;3(12):952–964. doi:10.1038/nrn986
23. Pouget P. The cortex is in overall control of 'voluntary' eye movement. *Eye 2015 292*. 2014;29(2):241–245. doi:10.1038/eye.2014.284
24. Safron A, Klimaj V, Hipólito I. On the Importance of Being Flexible: Dynamic Brain Networks and Their Potential Functional Significances. *Front Syst Neurosci*. 2022;15:688424. doi:10.3389/FNSYS.2021.688424/FULL

25. Zarghami TS, Friston KJ. Dynamic effective connectivity. *Neuroimage*. 2020;207:116453. doi:10.1016/J.NEUROIMAGE.2019.116453
26. Kim J, Criaud M, Cho SS, et al. Abnormal intrinsic brain functional network dynamics in Parkinson's disease. *Brain*. 2017;140(11):2955–2967. doi:10.1093/BRAIN/AWX233
27. Klobušiakova P, Mareček R, Fousek J, Výtvarova E, Rektorova I. Connectivity between Brain Networks Dynamically Reflects Cognitive Status of Parkinson's Disease: A Longitudinal Study. *J Alzheimer's Dis*. 2019;67(3):971–984. doi:10.3233/JAD-180834;ISSUE:ISSUE:DOI
28. Zhu J, Zeng Q, Shi Q, et al. Altered Brain Functional Network in Subtypes of Parkinson's Disease: A Dynamic Perspective. *Front Aging Neurosci*. 2021;13:710735. doi:10.3389/FNAGI.2021.710735/TEXT
29. Kim J, Criaud M, Cho SS, et al. Abnormal intrinsic brain functional network dynamics in Parkinson's disease. *Brain*. 2017;140(11):2955–2967. doi:10.1093/brain/awx233
30. Engels G, Vlaar A, McCoy B, Scherder E, Douw L. Dynamic Functional Connectivity and Symptoms of Parkinson's Disease: A Resting-State fMRI Study. *Front Aging Neurosci*. 2018;10. doi:10.3389/FNAGI.2018.00388
31. Shaikh AG, Ghasia FF. Saccades in Parkinson's disease: Hypometric, slow, and maladaptive. In: *Progress in Brain Research*. Vol 249. Elsevier; 2019:81–94. doi:10.1016/bs.pbr.2019.05.001
32. MacAskill MR, Anderson TJ, Jones RD. Adaptive modification of saccade amplitude in Parkinson's disease. *Brain*. 2002;125(7):1570–1582. doi:10.1093/brain/awf168
33. Chan F, Armstrong IT, Pari G, Riopelle RJ, Munoz DP. Deficits in saccadic eye-movement control in Parkinson's disease. *Neuropsychologia*. 2005;43(5):784–796. doi:10.1016/J.NEUROPSYCHOLOGIA.2004.06.026
34. Camacho PB, Carbonari R, Shen S, Zadikoff C, Kramer AF, López-Ortiz C. Voluntary saccade training protocol in persons with Parkinson's disease and healthy adults. *Front Aging Neurosci*. 2019;11(APR):441242. doi:10.3389/FNAGI.2019.00077/TEXT
35. Srivastava A, Sharma R, Sood SK, Shukla G, Goyal V, Behari M. Saccadic eye movements in Parkinson's disease. *Indian J Ophthalmol*. 2014;62(5):538–544. doi:10.4103/0301-4738.133482
36. Chambers JM, Prescott TJ. Response times for visually guided saccades in persons with Parkinson's disease: A meta-analytic review. *Neuropsychologia*. 2010;48(4):887–899. doi:10.1016/j.neuropsychologia.2009.11.006
37. Pah ND, Ngo QC, McConnell N, et al. Reflexive eye saccadic parameters in Parkinson's disease. *Front Med Technol*. 2024;6:1477502. doi:10.3389/fmedt.2024.1477502
38. Waldthaler J, Tsitsi P, Svenningsson P. Vertical saccades and antisaccades: complementary markers for motor and cognitive impairment in Parkinson's disease. *npj Park Dis*. 2019;5(1):11-. doi:10.1038/s41531-019-0083-7
39. Waldthaler J, Stock L, Krüger-Zechlin C, Deeb Z, Timmermann L. Cluster analysis reveals distinct patterns of saccade impairment and their relation to cognitive profiles in Parkinson's disease. *J Neuropsychol*. 2023;17(2):251–263. doi:10.1111/jnp.12302
40. Waldthaler J, Stock L, Student J, Sommerkorn J, Dowiasch S, Timmermann L. Antisaccades in Parkinson's Disease: A Meta-Analysis. *Neuropsychol Rev 2021 314*. 2021;31(4):628–642. doi:10.1007/S11065-021-09489-1
41. Munoz MJ, Reilly JL, Pal GD, et al. Medication adversely impacts visually-guided eye movements in Parkinson's disease. *Clin Neurophysiol*. 2022;143:145–153. doi:10.1016/j.clinph.2022.07.505
42. Lu Z, Buchanan T, Kennard C, FitzGerald JJ, Antoniades CA. The effect of levodopa on saccades – Oxford Quantification in Parkinsonism study. *Park Relat Disord*. 2019;68:49–56. doi:10.1016/j.parkreldis.2019.09.029
43. Díez-Cirarda M, Strafella AP, Kim J, et al. Dynamic functional connectivity in Parkinson's disease patients with mild cognitive impairment and normal cognition. *NeuroImage Clin*. 2018;17:847–855. doi:10.1016/j.nicl.2017.12.013
44. LeWitt PA, Chaudhuri KR. Unmet needs in Parkinson disease: Motor and non-motor. *Parkinsonism Relat Disord*. 2020;80:S7-S12. doi:10.1016/J.PARKRELDIS.2020.09.024
45. Alves G, Wentzel-Larsen T, Aarsland D, Larsen JP. Progression of motor impairment and disability in Parkinson disease. *Neurology*. 2005;65(9):1436–1441. doi:10.1212/01.WNL.0000183359.50822.F2
46. Post B, Muslimovic D, van Geloven N, Speelman JD, Schmand B, de Haan RJ. Progression and prognostic factors of motor impairment, disability and quality of life in newly diagnosed Parkinson's disease. *Mov Disord*. 2011;26(3):449–456. doi:10.1002/MDS.23467
47. Tahmasian M, Eickhoff SB, Giehl K, et al. Resting-state functional reorganization in Parkinson's disease: An activation likelihood estimation meta-analysis. *Cortex*. 2017;92:119–138. doi:10.1016/j.cortex.2017.03.016
48. Lemos J, Pereira D, Almendra L, et al. Distinct functional properties of the vertical and horizontal saccadic network in Health and Parkinson's disease: An eye-tracking and fMRI study. *Brain Res*. 2016;1648(4):469–484. doi:10.1016/j.brainres.2016.07.037
49. Gorges M, Müller HP, Lulé D, et al. The association between alterations of eye movement control and cerebral intrinsic functional connectivity in Parkinson's disease. *Brain Imaging Behav*. 2016;10(1):79–91. doi:10.1007/s11682-015-9367-7
50. Gorges M, Müller HP, Kassubek J. Structural and functional brain mapping correlates of impaired eye movement control in parkinsonian syndromes: A systems-based concept. *Front Neurol*. 2018;9(MAY):350506. doi:10.3389/fneur.2018.00319
51. Gratton C, Koller JM, Shannon W, et al. Emergent Functional Network Effects in Parkinson Disease. *Cereb Cortex*. 2019;29(6):2509–2523. doi:10.1093/CERCOR/BHY121

52. Baggio HC, Sala-Llonch R, Segura B, et al. Functional brain networks and cognitive deficits in Parkinson's disease. *Hum Brain Mapp*. 2014;35(9):4620–4634. doi:10.1002/HBM.22499;SUBPAGE:STRING:ABSTRACT;WEBSITE:WEBSITE:PERICLES;REQUESTEDJOURNAL:JOURNAL:10970193;ISSUE:ISSUE:DOI
53. Ko JH, Spetsieris PG, Eidelberg D. Network Structure and Function in Parkinson's Disease. *Cereb Cortex*. 2018;28(12):4121–4135. doi:10.1093/CERCOR/BHX267
54. Si Q, Gan C, Zhang H, et al. Altered dynamic functional network connectivity in levodopa-induced dyskinesia of Parkinson's disease. *CNS Neurosci Ther*. 2023;29(1):192–201. doi:10.1111/cns.13994
55. Hensel L, Seger A, Farrher E, et al. Fronto-striatal dynamic connectivity is linked to dopaminergic motor response in Parkinson's disease. *Park Relat Disord*. 2023;114. doi:10.1016/j.parkreldis.2023.105777
56. Gaymard B. Cortical and sub-cortical control of saccades and clinical application. *Rev Neurol (Paris)*. 2012;168(10):734–740. doi:10.1016/J.NEUROL.2012.07.016
57. Sparks DL. The brainstem control of saccadic eye movements. *Nat Rev Neurosci 2002 312*. 2002;3(12):952–964. doi:10.1038/nrn986
58. Biondetti E, Gaurav R, Yahia-Cherif L, et al. Spatiotemporal changes in substantia nigra neuromelanin content in Parkinson's disease. *Brain*. 2020;143(9):2757–2770. doi:10.1093/brain/awaa216
59. Guadron L, van Opstal AJ, Goossens J. Speed-accuracy tradeoffs influence the main sequence of saccadic eye movements. *Sci Reports 2022 121*. 2022;12(1):5262-. doi:10.1038/s41598-022-09029-8
60. Grosbras MH, Laird AR, Paus T. Cortical regions involved in eye movements, shifts of attention, and gaze perception. *Hum Brain Mapp*. 2005;25(1):140. doi:10.1002/hbm.20145
61. Domagalik A, Beldzik E, Fafrowicz M, Oginska H, Marek T. Neural networks related to pro-saccades and anti-saccades revealed by independent component analysis. *Neuroimage*. 2012;62(3):1325–1333. doi:10.1016/j.neuroimage.2012.06.006
62. Gorges M, Müller HP, Lulé D, Ludolph AC, Pinkhardt EH, Kassubek J. Functional Connectivity Within the Default Mode Network Is Associated With Saccadic Accuracy in Parkinson's Disease: A Resting-State fMRI and Videooculographic Study. *Brain Connect*. 2013;3(3):265–272. doi:10.1089/brain.2013.0146
63. Matsuda T, Matsuura M, Ohkubo T, et al. Functional MRI mapping of brain activation during visually guided saccades and antisaccades: cortical and subcortical networks. *Psychiatry Res Neuroimaging*. 2004;131(2):147–155. doi:10.1016/j.pscychresns.2003.12.007
64. Linzenbold W, Lindig T, Himmelbach M. Functional neuroimaging of the oculomotor brainstem network in humans. *Neuroimage*. 2011;57(3):1116–1123. doi:10.1016/j.neuroimage.2011.05.052
65. Jamadar SD, Fielding J, Egan GF. Quantitative meta-analysis of fMRI and PET studies reveals consistent activation in fronto-striatal-parietal regions and cerebellum during antisaccades and prosaccades. *Front Psychol*. 2013;4(OCT):61341. doi:10.3389/fpsyg.2013.00749
66. Hwang K, Velanova K, Luna B. Strengthening of Top-Down Frontal Cognitive Control Networks Underlying the Development of Inhibitory Control: A Functional Magnetic Resonance Imaging Effective Connectivity Study. *J Neurosci*. 2010;30(46):15535–15545. doi:10.1523/JNEUROSCI.2825-10.2010
67. Zhou W, Shu H. A meta-analysis of functional magnetic resonance imaging studies of eye movements and visual word reading. *Brain Behav*. 2017;7(5):e00683. doi:10.1002/brb3.683
68. Fuchs AF, Kaneko CRS, Scudder CA. Brainstem control of saccadic eye movements. *Annu Rev Neurosci*. 1985;8(1):307–337. doi:10.1146/annurev.ne.08.030185.001515
69. Tanaka M, Kunimatsu J. Contribution of the central thalamus to the generation of volitional saccades. *Eur J Neurosci*. 2011;33(11):2046–2057. doi:10.1111/j.1460-9568.2011.07699.x
70. Pouget P. The cortex is in overall control of 'voluntary' eye movement. *Eye 2015 292*. 2014;29(2):241–245. doi:10.1038/eye.2014.284
71. Kheradmand A, Zee DS. Cerebellum and ocular motor control. *Front Neurol*. 2011;SEP:11499. doi:10.3389/fneur.2011.00053
72. Coiner B, Pan H, Bennett ML, et al. Functional neuroanatomy of the human eye movement network: a review and atlas. *Brain Struct Funct 2019 2248*. 2019;224(8):2603–2617. doi:10.1007/s00429-019-01932-7
73. Hikosaka O, Takikawa Y, Kawagoe R. Role of the basal ganglia in the control of purposive saccadic eye movements. *Physiol Rev*. 2000;80(3):953–978. doi:10.1152/physrev.2000.80.3.953
74. Preti MG, Bolton TA, Van De Ville D. The dynamic functional connectome: State-of-the-art and perspectives. *Neuroimage*. 2017;160(4):41–54. doi:10.1016/j.neuroimage.2016.12.061
75. Leonardi N, Van De Ville D. On spurious and real fluctuations of dynamic functional connectivity during rest. *Neuroimage*. *Academic Press Inc.* 2015;104:430–436. doi:10.1016/j.neuroimage.2014.09.007
76. Mamashli F, Hämäläinen M, Ahveninen J, Kenet T, Khan S. Permutation Statistics for Connectivity Analysis between Regions of Interest in EEG and MEG Data. *Sci Reports 2019 91*. 2019;9(1):7942-. doi:10.1038/s41598-019-44403-z
77. Toppi J, De Vico Fallani F, Petti M, et al. A new statistical approach for the extraction of adjacency matrix from effective connectivity networks. *Proc Annu Int Conf IEEE Eng Med Biol Soc EMBS*. Published online 2013:2932–2935. doi:10.1109/EMBC.2013.6610154
78. Kadhim MN, Al-Shammary D, Mahdi AM, Ibaida A. Feature selection based on Mahalanobis distance for early Parkinson disease classification. *Comput Methods Programs Biomed Updat*. 2025;7(12):100177. Accessed December 14, 2025.

https://www.sciencedirect.com/science/article/pii/S2666990025000011

79. Statistics PMSTIJ of, A S, 2018 undefined. On the generalized distance in statistics. *JSTOR*. Accessed February 17, 2026. https://www.jstor.org/stable/48723335
80. Baldereschi M, Di Carlo A, Rocca WA, et al. Parkinson's disease and parkinsonism in a longitudinal study: two-fold higher incidence in men. *Neurol Baldereschi, A Di Carlo, WA Rocca*, P Vanni, S Maggi, E Perissinotto, *F GrigolettoNeurology, 2000•neurology.org*. 2000;55(9):1358–1363. doi:10.1212/WNL.55.9.1358
81. Wooten GF, Currie LJ, Bovbjerg VE, Lee JK, Patrie J. Are men at greater risk for Parkinson's disease than women? *J Neurol Neurosurg Psychiatry*. 2004;75(4):637–639. doi:10.1136/jnnp.2003.020982
82. Morel P, Baraduc P. Dissociating the impact of sensory and motor noise in human saccades.*Cinquième conférence plénière …*. Published online 2010. http://hal.archives-ouvertes.fr/hal-00553434/
83. Apker GA, Darling TK, Buneo CA. Interacting noise sources shape patterns of arm movement variability in three-dimensional space. *J Neurophysiol*. 2010;104(5):2654–2666. doi:10.1152/jn.00590.2010
84. Van Beers RJ, Haggard P, Wolpert DM. The Role of Execution Noise in Movement Variability. *J Neurophysiol*. 2004;91(2):1050–1063. doi:10.1152/jn.00652.2003
85. Zilles K, Amunts K. Individual variability is not noise. *Trends Cogn Sci*. 2013;17(4):153–155. doi:10.1016/j.tics.2013.02.003
86. Zhu H, Huang J, Deng L, et al. Abnormal dynamic functional connectivity associated with subcortical networks in Parkinson's disease: A temporal variability perspective. *Front Neurosci*. 2019;13(FEB):1–13. doi:10.3389/fnins.2019.00080
87. Menon SS, Krishnamurthy K. A Comparison of Static and Dynamic Functional Connectivities for Identifying Subjects and Biological Sex Using Intrinsic Individual Brain Connectivity. *Sci Rep*. 2019;9(1). doi:10.1038/s41598-019-42090-4
88. Nemanich ST, Earhart GM. Freezing of gait is associated with increased saccade latency and variability in Parkinson's disease. *Clin Neurophysiol*. 2016;127(6):2394–2401. doi:10.1016/j.clinph.2016.03.017
89. Antoniades CA, Spering M. Eye movements in Parkinson's disease: from neurophysiological mechanisms to diagnostic tools. *Trends Neurosci*. 2024;47(1):71–83. doi:10.1016/j.tins.2023.11.001
90. Shaikh AG, Ghasia FF. *Saccades in Parkinson's Disease: Hypometric, Slow, and Maladaptive*. Vol 249. 1st ed. Elsevier B.V.; 2019. doi:10.1016/bs.pbr.2019.05.001
91. Bartz AE. Eyemovement latency, duration, and response time as a function of angular displacement. *J Exp Psychol*. 1962;64(3):318–324. doi:10.1037/h0043475
92. Srivastava A, Sharma R, Sood SK, Shukla G, Goyal V, Behari M. Saccadic eye movements in Parkinson's disease. *Indian J Ophthalmol*. 2014;62(5):538–544. doi:10.4103/0301-4738.133482
93. Jensen K, Beylergil SB, Shaikh AG. Slow saccades in cerebellar disease. *Cerebellum Ataxias 2019 61*. 2019;6(1):1-. doi:10.1186/s40673-018-0095-9
94. Terao Y, Fukuda H, Hikosaka O. What do eye movements tell us about patients with neurological disorders? — An introduction to saccade recording in the clinical setting —. *Proc Japan Acad Ser B*. 2017;93(10):772–801. doi:10.2183/pjab.93.049
95. Sangare A, de Liège A, Gaymard B, et al. Ocular Motor Abnormalities in Functional Neurological Disorder: A Video-Oculography Study. *Mov Disord Clin Pract*. Published online October 15, 2025. doi:10.1002/mdc3.70394
96. Winograd-Gurvich CT, Georgiou-Karistianis N, Evans A, et al. Hypometric primary saccades and increased variability in visually-guided saccades in Huntington's disease. *Neuropsychologia*. 2003;41(12):1683–1692. doi:10.1016/S0028-3932(03)00096-4
97. Sheridan MR, Flowers KA. Movement variability and bradykinesia in parkinson's disease. *Brain*. 1990;113(4):1149–1161. doi:10.1093/brain/113.4.1149
98. Barbe MT, Amarell M, Snijders AH, et al. Gait and upper limb variability in Parkinson's disease patients with and without freezing of gait. *J Neurol 2013 2612*. 2013;261(2):330–342. doi:10.1007/s00415-013-7199-1
99. Moon Y, Sung JH, An R, Hernandez ME, Sosnoff JJ. Gait variability in people with neurological disorders: A systematic review and meta-analysis. *Hum Mov Sci*. 2016;47(6):197–208. doi:10.1016/j.humov.2016.03.010
100. Heiderscheit BC, Heiderscheit BC. Movement Variability as a Clinical Measure for Locomotion. *J Appl Biomech*. 2000;16(4):419–427. doi:10.1123/jab.16.4.419
101. Tessitore A, Amboni M, Esposito F, et al. Resting-state brain connectivity in patients with Parkinson's disease and freezing of gait. *Park Relat Disord*. 2012;18(6):781–787. doi:10.1016/j.parkreldis.2012.03.018
102. Tessitore A, Cirillo M, De Micco R. Functional Connectivity Signatures of Parkinson's Disease. *J Parkinsons Dis*. 2019;9(4):637–652. doi:10.3233/JPD-191592
103. Baggio HC, Sala-Llonch R, Segura B, et al. Functional brain networks and cognitive deficits in Parkinson's disease. *Hum Brain Mapp*. 2014;35(9):4620–4634. doi:10.1002/hbm.22499
104. Zhu J, Zeng Q, Shi Q, et al. Altered Brain Functional Network in Subtypes of Parkinson's Disease: A Dynamic Perspective. *Front Aging Neurosci*. 2021;13:710735. doi:10.3389/FNAGI.2021.710735/BIBTEX

105. Ren J, Zhang W, Dahmani L, et al. Parkinson's disease as a somato-cognitive action network disorder. *Nat 2026*. Published online February 4, 2026:1–9. doi:10.1038/s41586-025-10059-1

106. Gorges M, Müller HP, Lulé D, et al. The association between alterations of eye movement control and cerebral intrinsic functional connectivity in Parkinson's disease. *Brain Imaging Behav*. 2016;10(1):79–91. doi:10.1007/s11682-015-9367-7

107. Ji GJ, Hu P, Liu TT, et al. Functional connectivity of the corticobasal ganglia–thalamocortical network in Parkinson disease: A systematic review and meta-analysis with cross-validation. *Radiology*. 2018;287(3):973–982. doi:10.1148/radiol.2018172183

108. Aarsland D, Brønnick K, Larsen JP, Tysnes OB, Alves G. Mild cognitive impairment disrupts attention network connectivity in Parkinson's disease: A combined multimodal MRI and meta-analytical study. *Neuropsychologia*. 2018;112(13):105–115. doi:10.1212/01.wnl.0000338632.00552.cb

109. Hacker CD, Perlmutter JS, Criswell SR, Ances BM, Snyder AZ. Resting state functional connectivity of the striatum in Parkinson's disease. *Brain*. 2012;135(12):3699–3711. doi:10.1093/brain/aws281

110. Wu T, Wang L, Chen Y, Zhao C, Li K, Chan P. Changes of functional connectivity of the motor network in the resting state in Parkinson's disease. *Neurosci Lett*. 2009;460(1):6–10. doi:10.1016/j.neulet.2009.05.046

111. Cao Y, Si Q, Tong R, Zhang X, Li C, Mao S. Abnormal dynamic functional connectivity changes correlated with non-motor symptoms of Parkinson's disease. *Front Neurosci*. 2023;17:1116111. doi:10.3389/fnins.2023.1116111

112. Engels G, Vlaar A, McCoy B, Scherder E, Douw L. Dynamic Functional Connectivity and Symptoms of Parkinson's Disease: A Resting-State fMRI Study. *Front Aging Neurosci*. 2018;10:399561. doi:10.3389/fnagi.2018.00388

113. Liu A, Chen X, Dan X, McKeown MJ, Wang ZJ. A Combined Static and Dynamic Model for Resting-State Brain Connectivity Networks. *IEEE J Sel Top Signal Process*. 2016;10(7):1172–1181. doi:10.1109/JSTSP.2016.2594949

114. Churchill L, Ignatavicius A, Konuri A, et al. Functional Magnetic Resonance Imaging (fMRI) Signatures of Progression and Phenoconversion in Prodromal Synucleinopathies. *Mov Disord*. 2025;40(12):2664–2677. doi:
10.
1002/MDS.70025;ISSUE:ISSUE:DOI

115. John YJ, Sawyer KS, Srinivasan K, Müller EJ, Munn BR, Shine JM. It's about time: Linking dynamical systems with human neuroimaging to understand the brain. *Netw Neurosci (Cambridge, Mass)*. 2022;6(4):960–979. doi:10.1162/netn_a_00230

116. Chen R, Singh M, Braver TS, Ching SN. Dynamical models reveal anatomically reliable attractor landscapes embedded in resting-state brain networks. *Imaging Neurosci (Cambridge, Mass)*. 2025;3. doi:10.1162/imag_a_00442

117. Dotan D, Pinheiro-Chagas P, Al Roumi F, Dehaene S. Decoding social decisions from movement kinematics. *iScience*. 2022;25(12):105550. doi:10.1016/j.tics.2019.10.002

118. Yoon T, Jaleel A, Ahmed AA, Shadmehr R. Saccade vigor and the subjective economic value of visual stimuli. https://doi.org/101152/jn007002019. 2020;123(6):2161–2172. doi:10.1152/jn.00700.2019

119. Reppert TR, Choi JES, Haith AM, Shadmehr R. Changes in saccade kinematics associated with the value and novelty of a stimulus. 2012 *46th Annu Conf Inf Sci Syst CISS 2012*. Published online 2012. doi:10.1109/CISS.2012.6310914

120. Seideman JA, Stanford TR, Salinas E. Saccade metrics reflect decision-making dynamics during urgent choices. *Nat Commun 2018 91*. 2018;9(1):2907-. doi:10.1038/s41467-018-05319-w

121. Jamadar SD, Egan GF, Calhoun VD, Johnson B, Fielding J. Intrinsic Connectivity Provides the Baseline Framework for Variability in Motor Performance: A Multivariate Fusion Analysis of Low- and High-Frequency Resting-State Oscillations and Antisaccade Performance. *Brain Connect*. 2016;6(6):505–517. doi:10.1089/brain.2015.0411

122. Waschke L, Kloosterman NA, Obleser J, Garrett DD. Behavior needs neural variability. *Neuron*. 2021;109(5):751–766. doi:10.1016/j.neuron.2021.01.023

123. Kim J, Criaud M, Cho SS, et al. Abnormal intrinsic brain functional network dynamics in Parkinson's disease. *Brain*. 2017;140(11):2955–2967. doi:10.1093/BRAIN/AWX233

124. Wood JL, Weintraub S, Coventry C, et al. Montreal Cognitive Assessment (MoCA) Performance and Domain-Specific Index Scores in Amnestic versus Aphasic Dementia. *J Int Neuropsychol Soc*. 2020;26(9):927. doi:10.1017/S135561772000048X

125. Ay U, Kicik A, Erdogdu E, et al. Beyond atrophy: Network-level functional disintegration pattern along the cognitive decline in Parkinson's disease. *Behav Brain Res*. 2026;511. doi:10.1016/j.bbr.2026.116289

126. Boon LI, Hepp DH, Douw L, et al. Functional connectivity between resting-state networks reflects decline in executive function in Parkinson's disease: A longitudinal fMRI study. *NeuroImage Clin*. 2020;28. doi:10.1016/j.nicl.2020.102468

127. Johansson ME, Toni I, Bloem BR, Helmich RC. Parkinson's disease progression is shaped by longitudinal changes in cerebral compensation. *Brain*. 2026;149(1):194–208. doi:10.1093/brain/awaf302

128. Terao Y, Fukuda H, Ugawa Y, Hikosaka O. New perspectives on the pathophysiology of Parkinson's disease as assessed by saccade performance: A clinical review. *Clin Neurophysiol*. 2013;124(8):1491–1506. doi:10.1016/j.clinph.2013.01.021

129. Termsarasab P, Thammongkolchai T, Rucker JC, Frucht SJ. The diagnostic value of saccades in movement disorder patients: a practical guide and review. *J Clin Mov Disord* 2015 *21*. 2015;2(1):14-. doi:10.1186/S40734-015-0025-4

130. Ramat S, Leigh RJ, Zee DS, Optican LM. What clinical disorders tell us about the neural control of saccadic eye movements. *Brain*. 2007;130(1):10–35. doi:10.1093/brain/awl309

131. Leigh RJ, Kennard C. Using saccades as a research tool in the clinical neurosciences. *Brain*. 2004;127(3):460–477. doi:10.1093/BRAIN/AWH035

132. Lage C, López-García S, Bejanin A, et al. Distinctive Oculomotor Behaviors in Alzheimer's Disease and Frontotemporal Dementia. *Front Aging Neurosci*. 2021;12:603790. doi:10.3389/fnagi.2020.603790

133. Ionescu A, Ștefănescu E, Strilciuc Ștefan, Grad DA, Mureșanu D. Eyes on dementia: an overview of the interplay between eye movements and cognitive decline. *J Med Life*. 2023;16(5):642. doi:10.25122/jml-2023-0217

134. Rane D, Dash DP, Dutt A, Dutta A, Das A, Lahiri U. Distinctive visual tasks for characterizing mild cognitive impairment and dementia using oculomotor behavior. *Front Aging Neurosci*. 2023;15:1125651. doi:10.3389/fnagi.2023.1125651

Figures

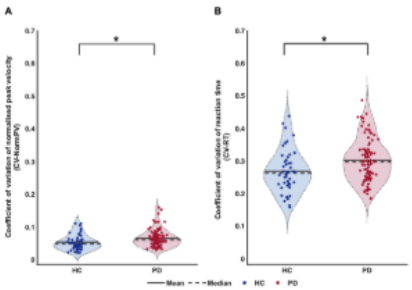


Figure 1

Group difference in the variability of saccadic behavioral parameters. Violin plots show the distribution of Coefficient of Variation (CV) values across participants in each group. **A.** CVs of normalized peak velocity, CV-NormPV. **B.** CVs of reaction time, CV-RT. Data are displayed in blue for healthy controls and in red for PD patients. The width of each violin reflects the density of observations, while individual points represent observations from individual participants. Solid and dashed horizontal lines denote the mean and median, respectively. Statistical thresholds for significant group differences are indicated by an asterisk ($*p_{Holm} < 0.05$).

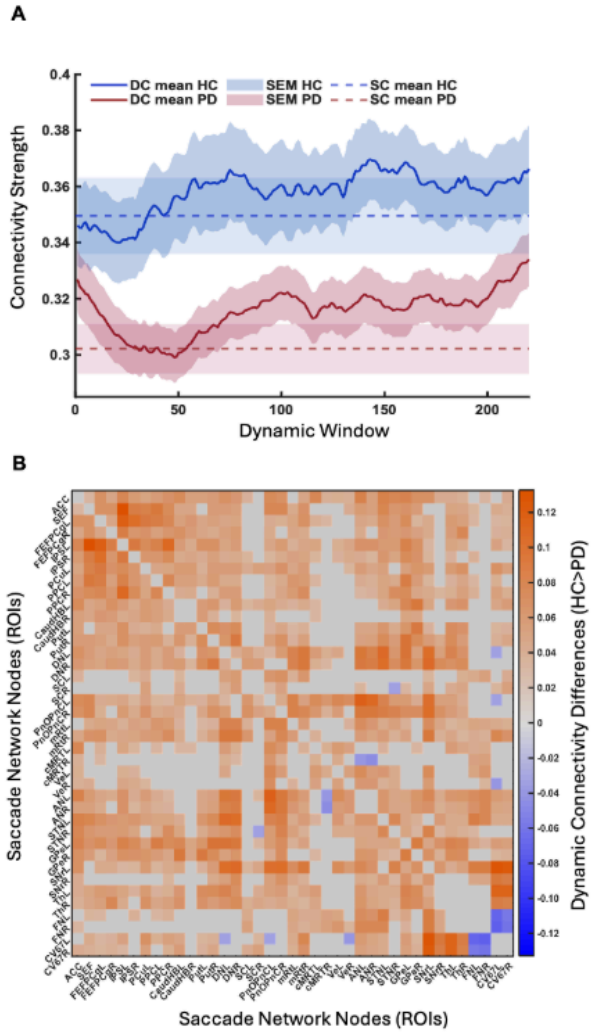


Figure 2

Group differences in functional connectivity. A. Static connectivity (SC; dashed lines) and dynamic connectivity (DC; solid, bold lines) are shown on a single graph to highlight differences between groups: in PD, both static and dynamic connectivity are lower than in HC. **B.** Dynamic connectivity matrix displaying the spread of group differences over the edges. The color bar shows the actual differences in Pearson correlation coefficients, and the gray edges are the non-significant ones after permutation testing.

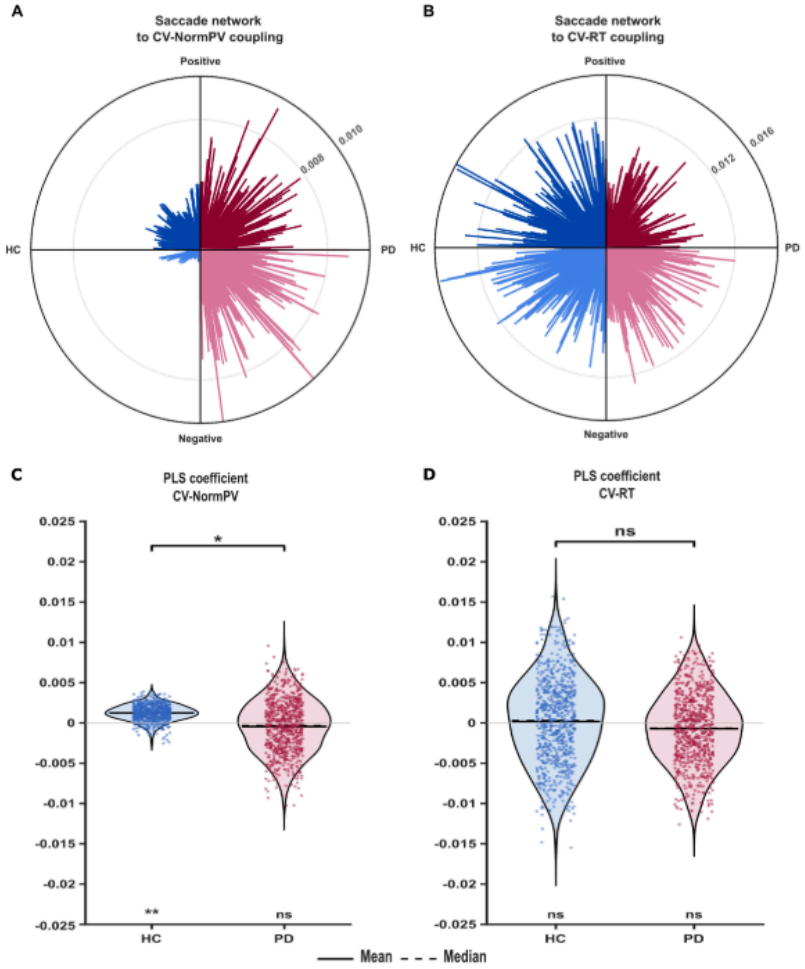


Figure 3

Coupling between dynamic connectivity in the saccadic network and saccadic variability. Network-behavior coupling was altered in PD compared to HC. For all the graphs, blue and red represent HC and PD, respectively. **A-B**. Radial maps depict the distribution of network-behavior coupling coefficients relating dynamic connectivity to saccadic variability: CV-NormPV (**A**) and CV-RT (**B**), with the values denoted next to each. Radial line length represents the magnitude of the PLS regression coefficient, with positive and negative coefficients shown in the upper and lower quadrants, respectively. **C-D**. Distributions of coupling coefficients between each edge (n=741) and saccadic variability for CV-NormPV (**C**) and CV-RT (**D**). Positive coefficients indicate that higher connectivity was associated with greater saccadic variability, and vice versa. Violin plots show the distribution of coefficients across edges (represented by points); solid and dashed lines represent the mean and median, respectively. Statistical significance is indicated at the top of the graph for between-group comparisons and at the bottom of the graph for within-group significance relative to zero (*p_{Holm} < 0.05, **p_{Holm} < 0.01; ns, not significant).

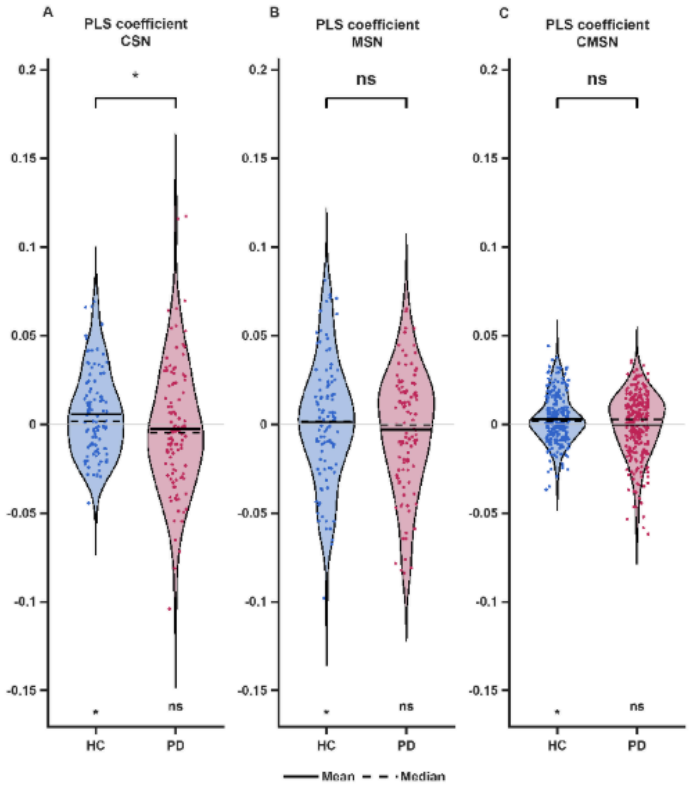


Figure 4

Specific contributions of cognitive and motor saccadic networks to saccadic behavior (CV-NormPV). Saccadic network-behavior coupling within and between the cognitive and motor networks was different between HC and PD, with significant differences in only the CSN. Violin plots show the distributions of coupling coefficients between network connectivity and saccadic variability (CV-NormPV) for the CSN (**A**), MSN (**B**), and CMSN (**C**) derived using a PLS regression model for each network. Blue and red colors represent HC and PD, respectively. Positive coefficients indicate that higher connectivity was associated with greater saccadic variability and vice versa. The plots depict the distribution of coupling coefficients across network edges (represented by points); solid and dashed horizontal lines represent the mean and median, respectively. Statistical significance is indicated at the top of the graph for between-group comparisons and at the bottom for within-group significance relative to zero (*p_{Holm} < 0.05, **p_{Holm} < 0.01; ns, not significant).

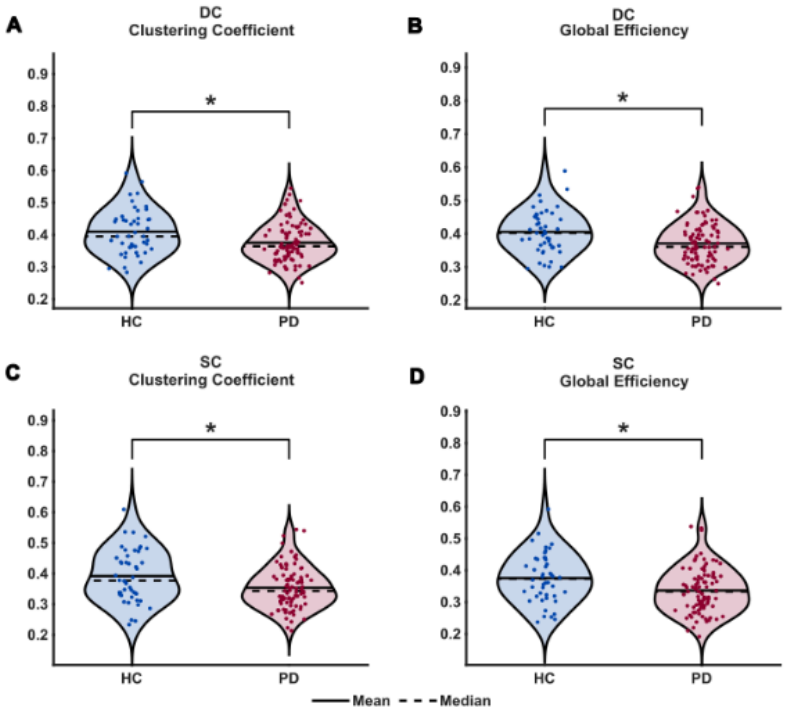


Figure 5

Network organization changes with PD. Violin plots show group differences in graph-theoretical network measures. **A-B.** Dynamic connectivity (DC). **C-D** Static connectivity (SC). **A, C:** Clustering coefficient. **B, D:** Global efficiency (right column). Healthy Controls (HC) = blue; Parkinson's disease patients (PD) = red. Individual points represent participants. Solid and dashed lines denote the mean and median, respectively. PD exhibited significantly lower clustering coefficient and global efficiency relative to HC across both DC and SC measures. Asterisks on the brackets at the top of the plots indicate between-group comparisons ($*p_{Holm} < 0.05$).

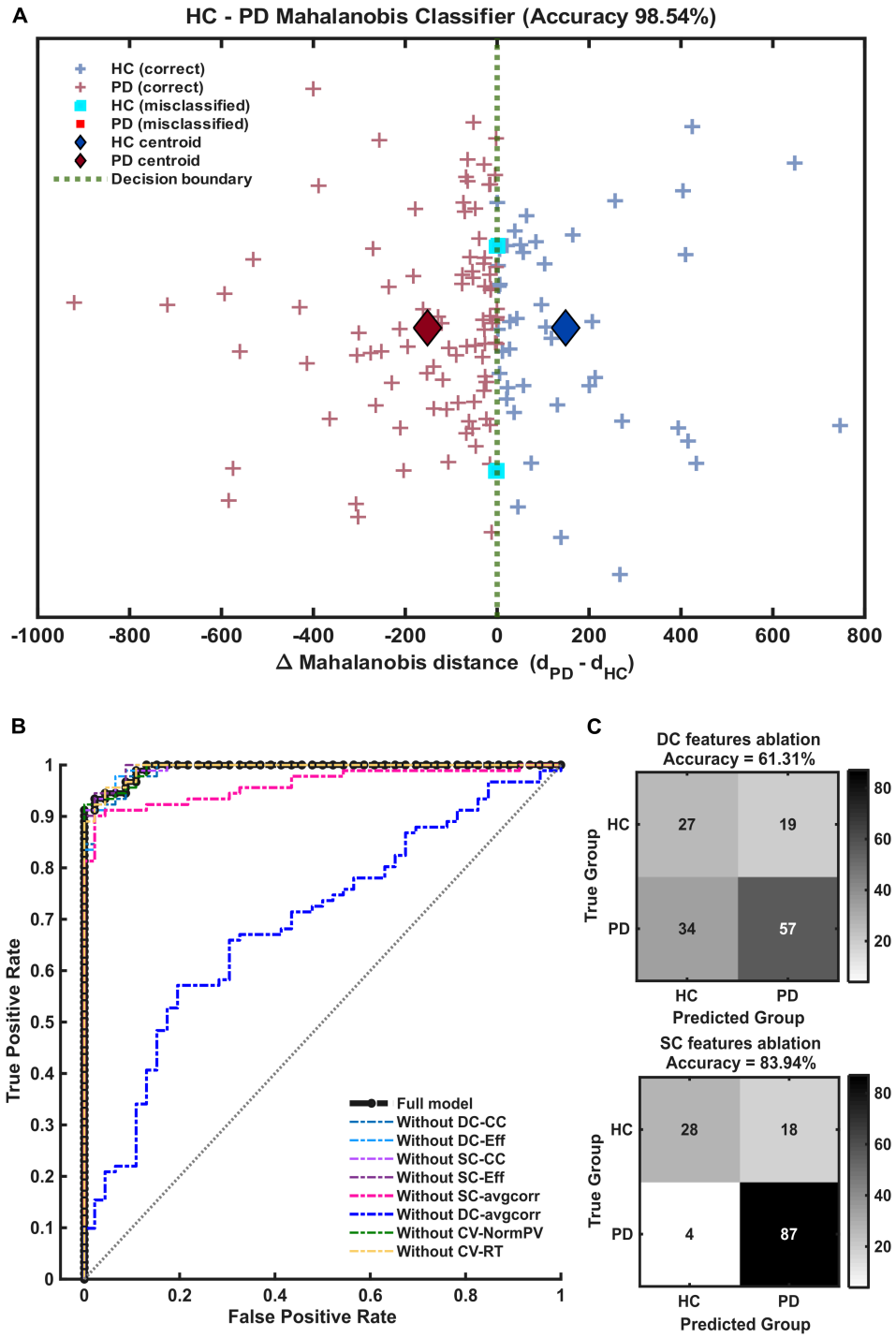


Figure 6

Classification of the population into healthy and PD groups using features derived from saccadic network connectivity and saccadic variability. A. Distribution of participants (each plus sign is a participant) over the manifold with HC (blue) and PD (red), showing misclassifications of two HCs (full cyan square) as PD, with an accuracy of 98.5%. Centroids of the groups are shown with filled diamonds. **B.** Classifier performance ROC curves with the full model in a bold black line, and an ablation analysis with each feature dropped, shown in different colors, showing that the ablation of the dynamic connectivity feature of the average correlation coefficient across ROIs has the maximum drop (blue dashed line). **C**. Leave-one-out classifier validation showing that the dynamic connectivity features ablation (lower panel), compared to static connectivity features (upper panel), has a greater effect on classification accuracy to separate PD from HC individuals.

Supplementary Files

This is a list of supplementary files associated with this preprint. Click to download.

- SupplementalNJPDICEBERGFINAL.docx